Journal of Geochemical Exploration 128 (2013) 51–61

Contents lists available at SciVerse ScienceDirect

Journal of Geochemical Exploration

journal homepage: www.elsevier.com/locate/jgeoexp

Geological and sulfur–lead–strontium isotopic studies of the Shaojiwan Pb–Zn deposit, southwest China: Implications for the origin of hydrothermal fluids

Jiaxi Zhou *, Zhilong Huang, Guangping Bao

State Key Laboratory of Ore Deposit Geochemistry, Institute of Geochemistry, Chinese Academy of Sciences, Guiyang 550002, PR China

ARTICLE INFO

Article history:
Received 17 August 2012
Accepted 16 January 2013
Available online 24 January 2013

Keywords:
S–Pb–Sr isotopes
Fluid mixing
Shaojiwan carbonate-hosted Pb–Zn deposit
SW China

ABSTRACT

Located on the western Yangtze Block, SW China, the Sichuan–Yunnan–Guizhou Pb–Zn metallogenic (SYG) province, contains known total Pb and Zn metals more than 20 million tons (Mt) grading >10% Pb + Zn and is a well known producer of base metals in China. The Shaojiwan carbonate-hosted Pb–Zn deposit is a representative deposit in this province with 0.5 Mt metals of 0.71 to 10.56% Pb and 2.09 to 30.27% Zn. Its ore bodies are hosted in Devonian and Permian carbonate rocks and structurally controlled by the Yadu–Mangdong thrust fault. Lead–zinc ores composed of pyrite, sphalerite, galena, calcite and dolomite occur as brecciated, veinlets and disseminations in dolomitized limestone rocks.

The S–Pb–Sr isotope compositions of sulfide minerals have been analyzed to trace the sources of sulfur and metals for the Shaojiwan Pb–Zn deposit. $\delta^{34}S$ values of sulfide minerals range from +8.4 to +11.6‰, suggesting that sulfur in the hydrothermal fluids was derived predominantly from evaporite rocks in the host strata. Sulfide minerals have a small range of Pb isotope compositions ($^{206}Pb/^{204}Pb = 18.616$ to 18.686, $^{207}Pb/^{204}Pb = 15.682$ to 15.728 and $^{208}Pb/^{204}Pb = 39.067$ to 39.181) that are close to upper crust Pb evolution curve and similar to Proterozoic basement in the SYG province. This implies that the lead metal originated mainly from the basement rocks. $^{87}Sr/^{86}Sr$ ratios of sphalerite range from 0.7114 to 0.7130, and $^{87}Sr/^{86}Sr_{200\ Ma}$ ratios range from 0.7113 to 0.7129, higher than Sinian to Permian sedimentary rocks and Permian Emeishan flood basalts, but lower than basement rocks. This implies a mixed strontium source between the older basement rocks and the younger cover sequences. Therefore, the fluids' mixing is a possible mechanism for sulfide precipitation in the Shaojiwan Pb–Zn deposit.

1. Introduction

Carbonate hosted Pb–Zn deposits are widely distributed around the world, including major districts in southeast Missouri, USA (Sverjensky, 1981), Pine Point, Canada (Powell and Macqueen, 1984), Upper Silesia in Europe (Wilkinson et al., 2005), and Sichuan, Yunnan and Guizhou (SYG) provinces in SW China (Leach et al., 2010; Zheng and Wang, 1991). The SYG Pb–Zn metallogenic province contains total Pb and Zn metals more than 20 million tons (Mt) at grades of >10% Pb + Zn (Table 1) and has been the major source of base metals in China (e.g., Cromie et al., 1996; Han et al., 2007; Zheng and Wang, 1991; Zhou et al., 2001). There are 408 Pb–Zn deposits of this type in the region, including the world class Huize Pb–Zn deposit (e.g., Han et al., 2007; Huang et al., 2003; Zhou et al., 2001), hosted in Sinian (Late Proterozoic) to Late Permian carbonate rocks (e.g., Cromie et al., 1996; Han et al., 2007; Liu and Lin, 1999; Zheng and Wang, 1991; Zhou et al., 2001, 2011, in press).

A close spatial association with Permian Emeishan flood basalts has been used to classify them as the distal magmatic–hydrothermal deposits (Xie, 1963). In addition, the Emeishan flood basalts were thought to be an important source of metals and heat (e.g., Han et al., 2007; Huang et al., 2003, 2010; Liu and Lin, 1999). On the other hand, these deposits have been interpreted as strata-bound and generated during the reworking of sedimentary rocks (Tu, 1984). Liao (1984) proposed a hypothesis of diverse sources of metals and thought that all Pb–Zn deposits in this region belonged to the same genetic type of hydrothermal deposits associated with post-diagenetic sulfate brines. However, other researchers have attributed the Pb–Zn deposits in the region to be Mississippi valley-type (MVT) deposits (e.g., Zheng and Wang, 1991; Zhou et al., 2001), with metals sourced from the carbonate host rocks (Jin, 2008) and Neoproterozoic igneous rocks (Zhou et al., 2001). Despite these controversies and a large number of publications in Chinese, it is still unclear how these metals became so highly concentrated in the SYG province.

S–Pb–Sr isotopes are powerful tool for fingerprinting ore-forming fluids and metals (e.g., Carr et al., 1995; Gromek et al., 2012; Haest et al., 2010; Huston et al., 1995; Wilkinson et al., 2005; Zheng and Wang, 1991; Zhou et al., 2001, 2010). In this paper, we describe the geology of the Shaojiwan Pb–Zn deposit in detail and report new S–Pb–Sr isotope

* Corresponding author at: Institute of Geochemistry, Chinese Academy of Sciences, Guanshui Road 46#, Guiyang 550002, PR China. Tel.: +86 851 5895900; fax: +86 851 5891664.
E-mail address: zhoujiaxi@vip.gyig.ac.cn (J. Zhou).

0375-6742/$ – see front matter © 2013 Elsevier B.V. All rights reserved.
http://dx.doi.org/10.1016/j.gexplo.2013.01.007

Table 1
Host strata, grade and tonnage of representative Pb–Zn deposits in the SYG province, SW China.

Deposits	Strata	Location	Metal association	Tonnage	Grade
Huize	C	Yunnan	Zn–Pb–Ge–Cd–Ag	>5 Mt	Pb + Zn > 25%
Maozu	S	Yunnan	Zn–Pb–Cd–Ag	>1 Mt	Pb + Zn > 12%
Maoping	D–C	Yunnan	Zn–Pb–Ag	>2 Mt	Pb + Zn > 25%
Fule	P	Yunnan	Zn–Pb–Cd–Ge–Ga–In	>0.4 Mt	Pb + Zn > 15%
Lemachang	D, P	Yunnan	Pb–Ag–Zn	>0.3 Mt	Pb + Zn > 10%
Tianbanshan	S	Sichuan	Zn–Pb–Cd–Ag	>1 Mt	Pb + Zn > 10%
Daliangzi	S	Sichuan	Zn–Pb–Ge–Cd–Ga–Ag	>1 Mt	Pb + Zn > 10%
Xiaoshifang	S	Sichuan	Zn–Pb–Cd–Ag	>1 Mt	Pb + Zn > 15%
Yinchanggou	S	Sichuan	Pb–Zn–Ag	>0.3 Mt	Pb + Zn > 14%
Paoma	S	Sichuan	Pb–Zn	>0.2 Mt	Pb + Zn > 10%
Tianqiao	D–C	Guizhou	Zn–Pb–Cd–Ag–Ge	>0.3 Mt	Pb + Zn > 15%
Yinchangpo	C	Guizhou	Pb–Zn–Ag–Ge	>0.2 Mt	Pb + Zn > 20%
Shanshulin	C	Guizhou	Zn–Pb–Ag–Cd–As	>0.5 Mt	Pb + Zn > 20%
Shaojiwan	D, P	Guizhou	Zn–Pb–Cd–Ag	>0.4 Mt	Pb + Zn > 15%
Maomaochang	C	Guizhou	Zn–Pb–Cd–Ag	>0.3 Mt	Pb + Zn > 12%
Zhazichang	C	Guizhou	Zn–Pb–Cd–Ag	>0.2 Mt	Pb + Zn > 10%
Qingshan	C	Guizhou	Zn–Pb–Cd–Ag–In	>0.3 Mt	Pb + Zn > 15%
Yadu	P	Guizhou	Zn–Pb–Cd–Ag	>0.5 Mt	Pb + Zn > 15%
Mangdong	D	Guizhou	Zn–Pb–Cd–Ag	>0.3 Mt	Pb + Zn > 15%

Note: P = Permian; C = Carboniferous; D = Devonian; S = Sinian. The Huize and Maoping deposits are from Han et al. (2007); the Maozu, Fule, Tianbanshan, Daliangzi, Xiaoshifang and Yinchanggou Pb–Zn deposits are from Zheng and Wang (1991); Liu and Lin (1999); Huang et al. (2004); other deposits are from Zhou et al. (in press) and Jin (2008).

data of sulfide minerals. This new dataset, together with previously published results, is utilized to constrain the sources of the ore-forming fluids and metals for the Shaojiwan Pb–Zn deposit, and providing evidence as to how these metals concentrated highly in the SYG province.

2. Geological background

The Yangtze Block is composed of ~2.9 to ~3.3 Ga crystalline basements (Qiu et al., 2000), Meso- to Neoproterozoic folded basements (Sun et al., 2009; Zhao et al., 2010) and Paleozoic to Mesozoic cover sequences. In the western Yangtze Block, the folded basement rocks include the ~1.7 Ga Dongchuan and ~1.1 Ga Kunyang Groups and equivalents (Sun et al., 2009; Zhao et al., 2010) that consist of greywackes, slates and other carbonaceous to siliceous sedimentary rocks. These rocks are overlain unconformably by shallow marine Paleozoic and Lower Mesozoic cover sequences (Yan et al., 2003). Jurassic to Cenozoic strata are composed entirely of continental sequences (Liu and Lin, 1999). A major feature of the western Yangtze Block is the mantle plume-derived Emeishan Large Igneous Province (ELIP), which covers an area of more than 250,000 km^2 (Zhou et al., 2002). This igneous province is dominantly composed of Emeishan flood basalts.

The Pb–Zn deposits in the western Yangtze Block (Fig. 1A) are distributed in a large triangular area of 170,000 km^2 in NE Yunnan, NW Guizhou and SW Sichuan (Liu and Lin, 1999). More than four hundred Pb–Zn deposits have been reported in the province (Liu and Lin, 1999). They are characterized by irregular ore bodies with simple mineralogy, weak wall-rock alteration and high Pb + Zn grades of ores (more than 10%; Table 1), usually associated with Ag, Ge, Cd, Ga and In (e.g., Han et al., 2007; Zhou et al., 2011). They are mainly hosted in Sinian to Permian carbonate rocks, which are below the Permian Emeishan flood basalts (e.g., Han et al., 2007; Zheng and Wang, 1991; Zhou et al., 2001, 2011).

In the SE SYG province, the cover sequence includes Devonian to Triassic sedimentary rocks and Permian Emeishan flood basalts (Fig. 1B). Diabase dykes, also probably associated with the ELIP, are locally present. The Devonian strata consist of sandstone, siltstone, limestone and dolostone, and the Carboniferous strata are composed of shale, limestone, and dolostone. The Early Permian sedimentary sequence consists of sandstone, shale, coal and limestone, all of which are overlain by Permian Emeishan flood basalt. The basalt is overlain by Late Permian sandstone, siltstone and coal measures. The Triassic strata are composed of siltstone, sandstone, dolostone and limestone. The Pb–Zn ore bodies are hosted in Devonian to Permian carbonate rocks and controlled by the NW-trending tectonic belts, particularly the Yadu–Mangdong (F_1) and Weining–Shuicheng (Fw-s) faults (Fig. 1B).

3. Geology of the Shaojiwan deposit

3.1. The host rocks

The Shaojiwan Pb–Zn deposit occurs in the NW-trending Yadu–Mangdong fault in the SE SYG province (Fig. 1B). The ore bodies occur mainly in a thrust fault (F_1) that marks the contract between the Lower Permian Qixia Formation in the structural footwall and the Middle Devonian Dushan Formation in the hanging wall (Fig. 2A). Although Devonian to Permian sedimentary rocks are present through the mining district, Carboniferous carbonate rocks are poorly exposed to the southwestern (Fig. 1B). The host rocks are mainly Qixia, Dushan and Longdongshui Formations limestone, dolomitic limestone and dolomite (Fig. 2A and B). The detailed features of exposed rocks in the Shaojiwan ore field are shown in Fig. 3.

3.2. Structures in the mining district

Multiple stages of NW-trending faults and folds constitute the pre-Mesozoic Yadu–Mangdong tectonic belt. The ore deposit is situated on the SE segment of the asymmetrical Yadu–Mangdong anticline, which trends 310°, with axial plane dipping to the SW. Exposed in the axial part of the anticline are Devonian sedimentary rocks, with the Carboniferous and Permian sedimentary rocks exposed on both the limbs. The rocks on the SW limb have a dip angle of 25° to 56°. As the NE limb was destroyed by the Yadu–Mangdong fault, only Permian carbonate rocks have been preserved. Both limbs are characterized by a number of second-ordered anticlines and synclines. The faults within the mining district are composed of a series of high-angle thrust faults, forming an imbricate thrust–nappe structure (Fig. 2B). The strike of the faults is consistent with that of the folds. These structure elements extend through the whole region and have a close spatial connection with Pb–Zn mineralization.

3.3. Ore body characteristics

The ore bodies are classified into two types–the steeply dipping vein echelon and the gently dipping strata–bound types (Fig. 2A and B). A

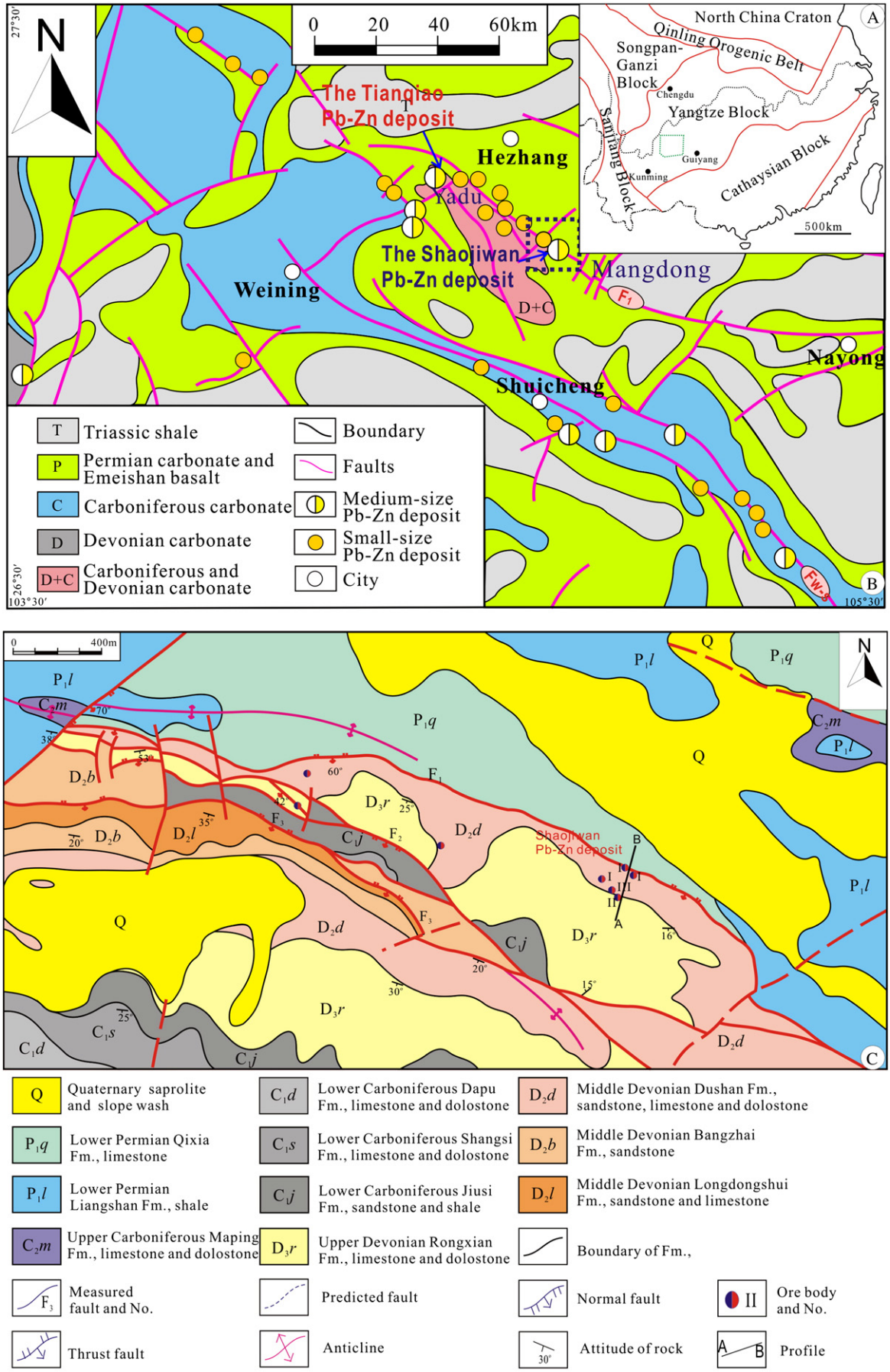

Fig. 1. A: regional geological setting; B: sketch geological map of NW Guizhou Pb–Zn metallogenic province; C: geological map of the Shaojiwan Pb–Zn deposit.

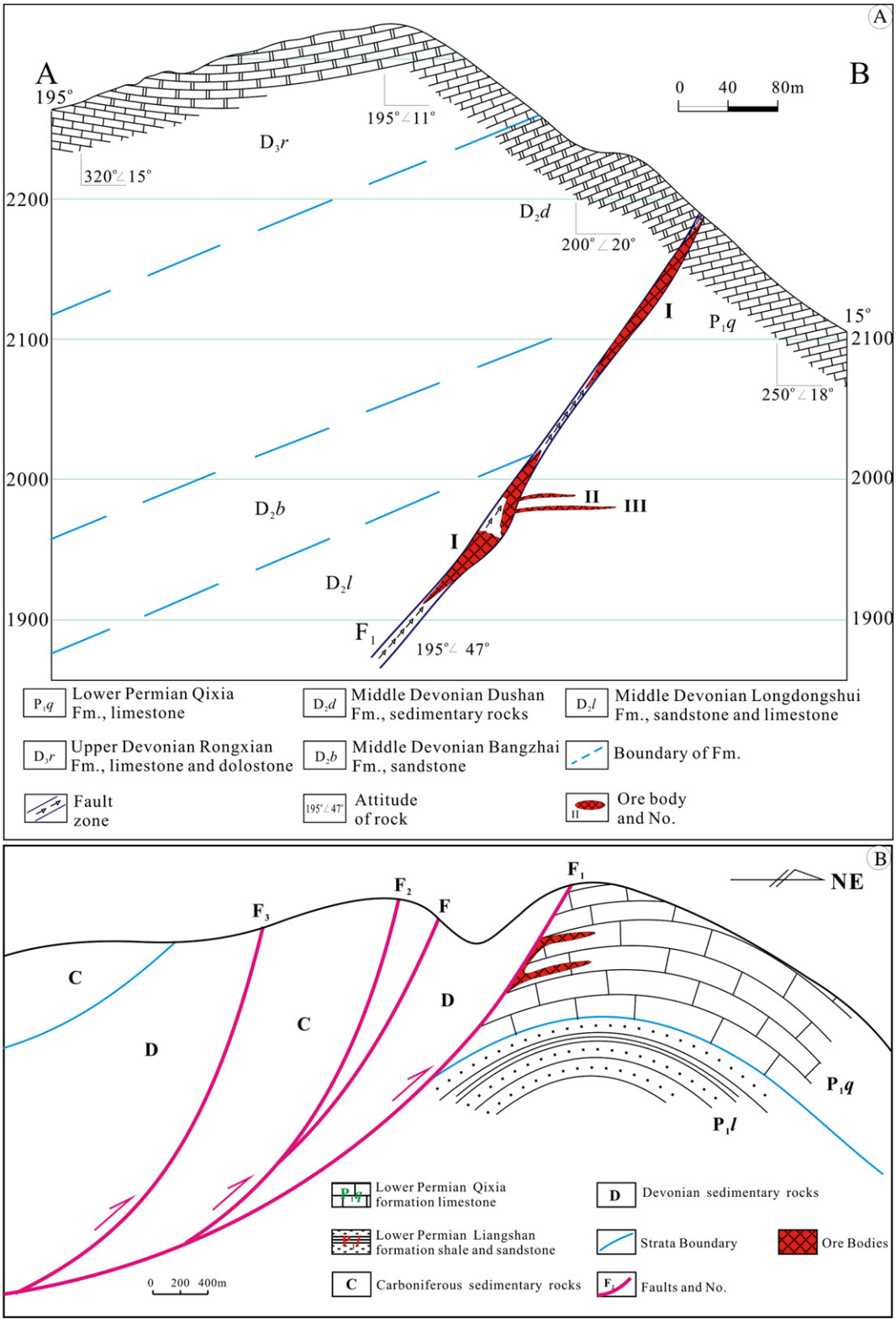

Fig. 2. A: A–B geological profile; B: sketch map of the imbricate thrust–nappe structure in the Shaojiwan Pb–Zn ore field.

total of three ore bodies have been delineated. The No. 1 ore body occurs in a fault zone and is steeply inclined, lenticular and veined in shape. The ore body is 360 m in length and extends down to 300 m. Above the water table, oxidized ores are dominant, whereas brecciated and massive sulfide ores are presented below. The Pb + Zn metals of this ore body exceed 0.4 Mt with Pb 0.71 to 10.56 wt.% (mean 3.37 wt.%) and Zn 2.09 to 30.27 wt.% (mean 11.68 wt.%). Both Nos. 2 and 3 ore bodies are located in the footwall of the F_1 fault (Fig. 2A and B). They are relatively small in scale and are hosted as massive Pb–Zn sulfides in the inter-layered tectonic between the Qixia Formation limestone and dolomitic limestone. The total Pb + Zn metals of Nos. 2 and 3 ore bodies more than 0.1 Mt with mean Pb + Zn grade of 18.42 wt.%. The results of

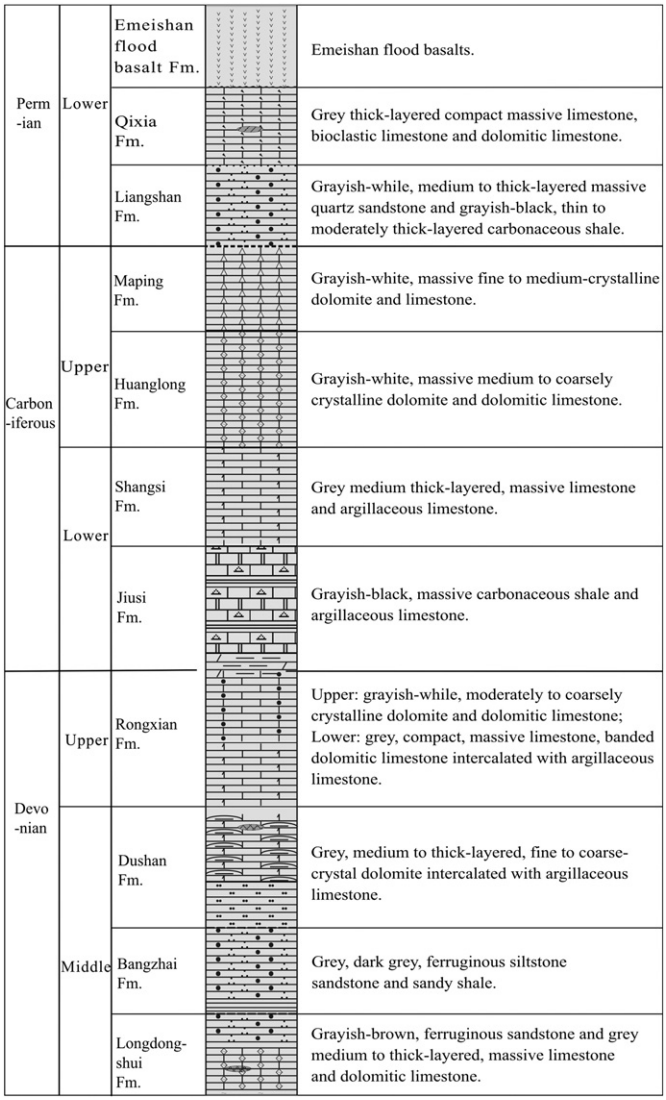

Fig. 3. The stratigraphic column of the Shaojiwan Pb–Zn deposit.

samples analysis indicated that in addition to Pb, Zn and Ag (19.9 to 384.9 ppm), the ores in this deposit also contain major amounts of Fe, Mg, As, and Sb and minor to trace elements of Cd, Ge, Ga, Se, In, Re and Tl (Zhou et al., 2011). Iron is present mainly in pyrite and subordinately in sphalerite and Fe–Mn carbonate rocks; Mn is present dominantly in Fe–Mn carbonate rocks; As, Sb and Re are present mainly in pyrite; Tl is present mainly in galena; and Ga, Ge, Cd, Se and In are present mainly in sphalerite.

3.4. Ore types and mineral composition

The ores from the Shaojiwan Pb–Zn deposit can be classified as three natural types: oxidized, mixed and sulfide ores. According to ore textures, the sulfide ores can be divided into massive, veinlets and disseminated ores. In accordance with the ore mineral paragenetic associations, ores of these types can be further divided into the sphalerite type (Fig. 4A), the galena type (Fig. 4B), the sphalerite–galena type (Fig. 4C and D), the sphalerite–calcite type (Fig. 4E), the sphalerite–galena–pyrite–calcite type (Fig. 4F), the galena–pyrite–calcite type (Fig. 4G) and the pyrite–calcite type (Fig. 4H), of which the sphalerite–galena type and galena–sphalerite–pyrite–calcite type are predominant. Primary ores in the deposit are dominated by coarse grained massive ores and are high grade. The oxidized ore minerals are extremely complicated in composition. More than ten minerals have been detected in oxidized ores, including cerussite, bonamite and limonite. Sulfide minerals are dominated by sphalerite, galena and pyrite and the main gangue minerals are calcite and dolomite, with a small amount of clay minerals.

3.5. Mineral characteristics

Sphalerite is the major ore mineral of the sphalerite, sphalerite–galena, sphalerite–calcite and sphalerite–pyrite–calcite assemblages, which occurs mainly as coarse-grained, xenomorphic–idiomorphic granular textures (Fig. 5). Sphalerite is mainly brown and less commonly brownish-yellow in color, and is 0.5 to 15 mm in grain size. Sphalerite occurs as massive, porphyritic, banded and disseminated aggregates commonly with interstitial galena, pyrite, calcite and other minerals (Fig. 5). Electron microprobe analyses indicate Fe contents of 1.94 to 2.75 wt.%.

The sphalerite contents of the other assemblages are relatively low. The sphalerite is fine- to moderately coarse-grained and has a xenomorphic–subidiomorphic granular texture. They are diverse in color, commonly brown and brownish-yellow, but occasionally pale yellow. The crystals are measured at 0.05 to 2 mm in grain size and mostly occur as porphyritic and disseminated aggregates in coexistence with galena, pyrite and calcite (Fig. 5). Sphalerite usually replaces pyrite to form skeletal crystals, exhibiting estuary, relic and poikilitic structures. Electron microprobe analyses of Fe contents are less than 1 wt.%.

Galena is another major mineral in the ores of the galena, sphalerite–galena, sphalerite–galena–pyrite–calcite and galena–pyrite–calcite assemblages (Fig. 4). In the galena and galena–pyrite–calcite assemblages, galena occurs as moderately coarse-grained (0.5 to 15 mm), subidiomorphic–idiomorphic grains that usually occur as aggregates in coexistence with sphalerite, pyrite and calcite, and cubic crystals are present. Galena often exhibits corrugation structure with pressure shadows. Variation of grain size and interpenetrating relationships indicate that this mineral crystallized over various stages. In the other types of ores the contents of galena are relatively low. The mineral occurs as fine to moderately coarse-grained (0.05 to 2 mm), xenomorphic–subidiomorphic granular textures. The galena mostly occurs as porphyritic and disseminated grains in coexistence with sphalerite, pyrite and calcite. It is also distributed, together with pyrite and calcite, in the interstices of sphalerite grains. Irregular galena is also distributed on the edges of relatively xenomorphic pyrite (Fig. 5).

Pyrite is the major sulfide mineral in the sphalerite–galena–pyrite–calcite, galena–pyrite–calcite and pyrite–calcite assemblages and also occurs in the wall rocks (Fig. 4). According to occurrence, crystal form and paragenetic mineral assemblage, three stages of pyrite can be distinguished. Pyrite of the early stage, which is present mainly in pyrite–calcite assemblages (Fig. 4H), has a cubic crystal form and occurs mostly as coarse to very coarse-grained granular texture, with a grain size up to 5 mm. Pyrite of the middle stage has a coarse-grained (2 to 5 mm), xenomorphic granular texture, but occurs mainly as pentagonal dodecahedral or cubic crystals that are usually present as disseminated and banded grains in the wall rocks near to ore bodies. Pyrite of the final stage has a sub-xenomorphic, xenomorphic or colloform texture and is dominated by pentagonal dodecahedral grains with a grain size of 0.05 to 1 mm. Pyrite of this stage is in coexistence with sphalerite, galena and calcite, usually distributed together with galena and calcite in the interstices of sphalerite grains (Fig. 5). Besides the pyrite–calcite ores, the other ore types all contain pyrite of this stage. Electron microprobe analysis shows that colloform pyrite contains arsenic with the range of 2.55 to 4.02 wt.%. Arsenic was considered to be present as nonstoichiometric substitutions in pyrite and its concentrations vary with pyrite's habit and the degree of recrystallization (Huston et al.,

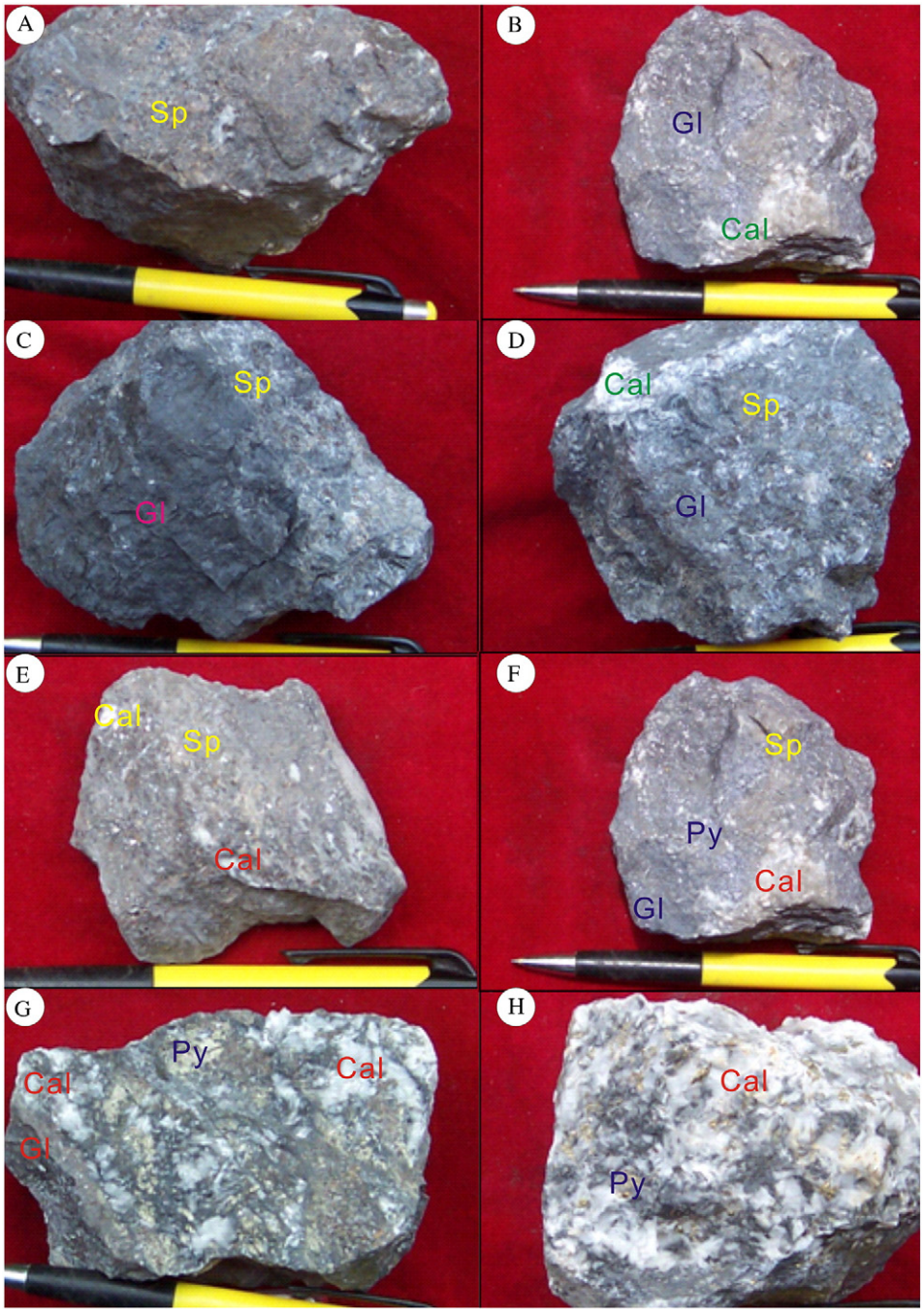

Fig. 4. Ore types of the Shaojiwan Pb–Zn deposit. A: sphalerite type; B: galena type; C–D: sphalerite–galena type; E: sphalerite–calcite type; F: galena–sphalerite–pyrite–calcite type; G: galena–pyrite–calcite type; H: pyrite–calcite type. Sp: sphalerite; Gl: galena; Py: pyrite; Cal: calcite.

1995; Large et al., 2000). The medium to high arsenic levels of colloform pyrite indicate that such pyrite relate to rapid precipitation at relative low temperature (Deol et al., 2012; Huston et al., 1995; Large et al., 2000; Ye et al., 2011).

Calcite is the main gangue mineral in the Shaojiwan Pb–Zn ore deposit. In oxidized and mixed ores, calcite has been mostly leached. In primary ores this mineral has four occurrences, i.e., massive, porphyritic, veined and filling. Massive calcite is irregular in form, generally larger than 10 cm in grain size, and has distinct boundaries with ore minerals (Fig. 4G and H). Porphyritic calcite is uniformly disseminated in ores. It is irregular grain in shape, mostly less than 2 cm in size, with indistinct boundaries to ore minerals. Calcite veins crosscut ore assemblages and are generally less than 2 cm in width. Irregular calcite fills the interstices of sphalerite together with brecciated pyrite (Figs. 5B and 5G–4J).

3.6. Wall rock alteration assemblages

Regional wall rock alterations include dolomitization, calcitization, Fe–Mn carbonatization and ferritization. Of these dolomitization and calcitization are closely associated with Pb–Zn mineralization. The hanging wall and foot wall of ore bodies are characterized by dolomitization and calcitization accompanied by recrystallization and decoloration. Fe–Mn carbonatization involves pale brown, reddish–brown and purple Fe-bearing dolomite. Although rarely observed at the Shaojiwan deposit, this assemblage is commonly present at the Maomaochang and Shanshulin Pb–Zn deposits. Fe–Mn carbonatization is a good indicator for ore prospecting, which is in association with Pb–Zn mineralization. Ferritization is present mainly as veinlets and irregular nodules in dolostone or as gossan resultant from pyrite oxidization. Its distribution

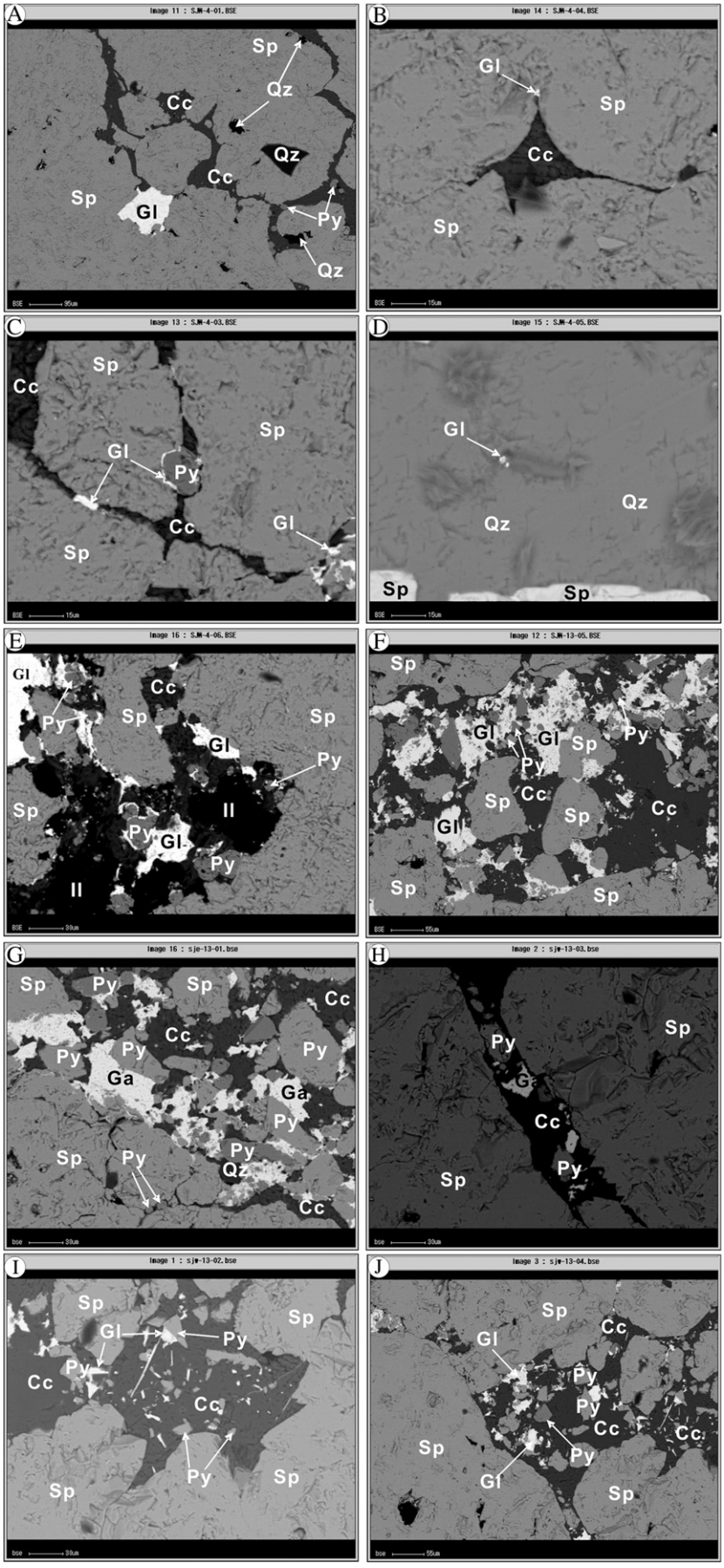

Fig. 5. EPMA photos of ores from the Shaojiwan Pb–Zn deposit. Sp: sphalerite; Gl: galena; Py: pyrite; Cal: calcite.

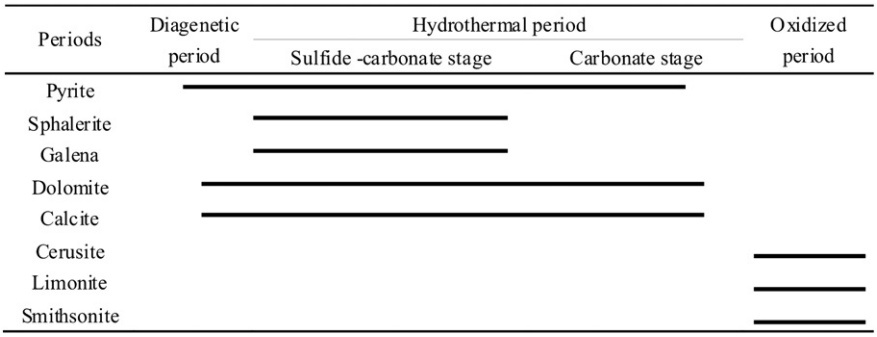

Fig. 6. Metallogenic stages and minerals-forming sequence of the Shaojiwan Pb–Zn deposit.

is not as extensive as dolomitization, but it is closely associated with Pb–Zn mineralization. The intensity of ferritization is always correlated with that of Pb–Zn mineralization.

3.7. Mineral paragenesis sequences

Based on the textures and structures, penetrating relations and mineral assemblages, the mineral sequences can be divided into diagenesis, hydrothermal and supergene periods (Fig. 6), of which the hydrothermal can further divided into two stages, i.e., the sulfide–carbonate and the carbonate stages. The sulfide–carbonate stage has a pyrite–massive calcite assemblage, a pyrite–sphalerite–porphyritic calcite assemblage and a sphalerite–galena–calcite vein assemblage.

4. Analytical methods

Samples representative the different ore types were taken from the main ore bodies of the Shaojiwan Pb–Zn deposit from both underground and drill cores. The samples were crushed as fine as 40 to 60 meshes, then pyrite, sphalerite and galena were picked out under the binocular microscope.

4.1. Sulfur isotopes

The sulfur isotope analyses were undertaken at the State Key Lab of Environmental Geochemistry, Institute of Geochemistry, Chinese Academy of Sciences, by using Continuous Flow Mass Spectrometer. GBW 04415 and GBW 04414 Ag_2S were used as the external standards and CDT as the reference standard, with the analytical accuracy of ± 0.1‰ (2σ).

4.2. Lead isotopes

Pb isotope analyses were carried out using the GV Isoprobe-T thermal ionization mass spectrometer at the Beijing Institute of Uranium Geology. The analytical procedure involved dissolution of samples using HF and $HClO_4$ in crucibles, followed by basic anion exchange resin to purify Pb. Analytical results for the standard NBS 981 are $^{208}Pb/^{204}Pb = 36.611 \pm 0.004$ (2σ), $^{207}Pb/^{204}Pb = 15.457 \pm 0.002$ (2σ) and $^{206}Pb/^{204}Pb = 16.937 \pm 0.002$ (2σ), in agreement with the referenced value (Belshaw et al., 1998).

Table 2
S isotope compositions of sulfide minerals from the Shaojiwan Pb–Zn deposit.

No.	Ore types	Object	$\delta^{34}S_{CDT}$/‰	Source
SJW-9-1	Gal + Py + Cal type	Py	11.4	Zhang et al. (2011)
SJW-15-1	Sp + Gal + Py + Cal type	Py	11.3	
SJW-14	Gal + Py + Cal type	Py	11.6	
SJW-12	Sp + Gal + Cal type	Gal	8.4	
SJW-1	Sp + Gal type	Brown Sp	11.1	
SJW-6	Gal + Py + Cal type	Brown Sp	11.1	
SJW-7	Sp + Gal + Cal type	Brown yellow Sp	10.1	This paper
SJW-11	Sp + Gal + Cal type	Light yellow Sp	9.8	
SJW-9-2	Gal + Py + Cal type	Brown yellow Sp	10.3	
SJW-15-2	Sp + Gal + Py + Cal type	Light yellow Sp	9.8	
SJW-16	Sp + Gal + Cal type	Brown yellow Sp	10.1	

Note: Gal = galena; Py = pyrite; Sp = sphalerite; Cal = calcite; SJW-9-1 and SJW-9-2 were taken from sample SJW-9, and SJW-15-1 and SJW-15-2 were taken from sample SJW-15.

4.3. Strontium isotopes

Chemical separation of Rb and Sr from matrix elements, and mass spectrometric measurement were accomplished in the Institute of Geology and Geophysics, Chinese Academy of Sciences. A detailed analytical procedure for Rb–Sr isotope analyses is available in Li et al. (2005). Spec-Sr exchange resin was used for the separation and purification of Rb and Sr. The whole procedure blank of Rb and Sr was about 6 pg. Isotopic compositions were measured by the Isoprobe-T TIMS. $^{87}Sr/^{86}Sr$ ratio of 8.37521 was used to calibrate instrument mass fractionation of strontium isotopes. The average $^{87}Sr/^{86}Sr$ ratio of NBS 987

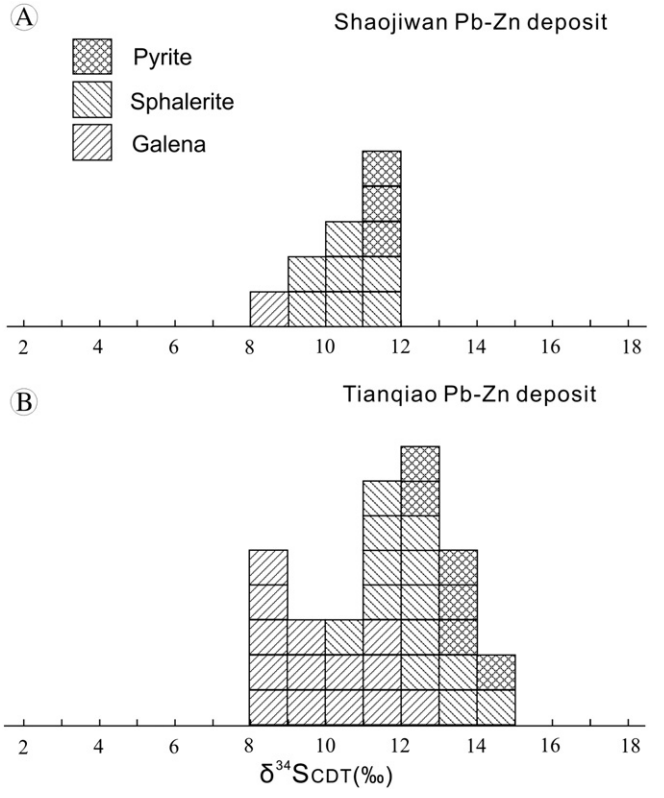

Fig. 7. S isotope composition histogram of the Shaojiwan Pb–Zn deposit (A) and S isotope composition histogram of the Tianqiao Pb–Zn deposit (B). The S isotope compositions of the Tianqiao Pb–Zn deposit are taken from Zhou et al. (in press).

Table 3
Pb isotope compositions of sulfide minerals from the Shaojiwan Pb–Zn deposit.

No.	Ore types	Object	$^{206}Pb/^{204}Pb$ (2σ)	$^{207}Pb/^{204}Pb$ (2σ)	$^{208}Pb/^{204}Pb$ (2σ)
SJW-14	Gal + Py + Cal type	Py	18.661 ± 0.002	15.714 ± 0.002	39.144 ± 0.005
SJW-9-1	Gal + Py + Cal type	Py	18.653 ± 0.003	15.708 ± 0.003	39.141 ± 0.007
SJW-15-1	Sp + Gal + Py + Cal type	Py	18.620 ± 0.003	15.694 ± 0.002	39.075 ± 0.006
SJW-9-2	Gal + Py + Cal type	Brown yellow Sp	18.686 ± 0.003	15.725 ± 0.002	39.179 ± 0.005
SJW-15-2	Sp + Gal + Py + Cal type	Light yellow Sp	18.671 ± 0.003	15.728 ± 0.002	39.181 ± 0.005
SJW-1	Sp + Gal type	Brown Sp	18.616 ± 0.003	15.682 ± 0.002	39.067 ± 0.006
SJW-12	Sp + Gal + Cal type	Gal	18.678 ± 0.002	15.719 ± 0.002	39.165 ± 0.004

Note: Gal = galena; Py = pyrite; Sp = sphalerite; Cal = calcite; SJW-9-1 and SJW-9-2 were taken from sample SJW-9, and SJW-15-1 and SJW-15-2 were taken from sample SJW-15. All data are from this study.

is 0.710242 ± 5 (n = 12). The uncertainties are 0.005% for Sr isotope compositions and 2% for $^{87}Rb/^{86}Sr$ ratios.

5. Analytical results

5.1. S isotope compositions

Sulfur isotope compositions of sulfide minerals (pyrite, sphalerite and galena) from the Shaojiwan Pb–Zn deposit are listed in Table 2. $\delta^{34}S$ values of sulfide minerals range from +8.4‰ to +11.6‰, with an average of +10.5‰ (Fig. 7A), similar to the Tianqiao deposit (Fig. 7B; Zhou et al., in press) in the same tectonic belt but 50 km away (Fig. 1B). Sphalerite has higher $\delta^{34}S$ values (+9.8‰ to +11.1‰) than galena (+8.4‰), but lower than pyrite (+11.3‰ to +11.6‰; Table 2). Sulfide minerals from the same sample have $\delta^{34}S_{pyrite} > \delta^{34}S_{sphalerite} > \delta^{34}S_{galena}$.

5.2. Pb–Sr isotope compositions

The Pb isotope compositions of sulfide minerals (pyrite, sphalerite and galena) are listed in Table 3 and Rb–Sr isotope compositions of sphalerite are listed in Table 4. $^{208}Pb/^{204}Pb$ ratios range from 39.067 to 39.181 (mean 38.136), $^{207}Pb/^{204}Pb$ ratios range from 15.682 to 15.728 (mean 15.710) and $^{206}Pb/^{204}Pb$ ratios range from 18.616 to 18.686 (mean 18.655). The $^{87}Sr/^{86}Sr$ ratios of sphalerite range from 0.7114 to 0.7130. Limited variations in Pb–Sr isotope compositions suggest that all the sulfide minerals have uniform Pb–Sr isotope sources.

6. Discussion

6.1. Possible sources of reduced sulfur

Primary ores from the Shaojiwan Pb–Zn deposit have simple sulfide mineralogy, including galena, sphalerite and pyrite, but lack sulfate minerals. Therefore, sulfide $\delta^{34}S$ approximates the hydrothermal fluid's $\delta^{34}S$ value (e.g., Basuki et al., 2008; Dixon and Davidson, 1996; Ohmoto et al., 1990; Seal, 2006). All of the ore minerals, including galena, sphalerite and pyrite, have $\delta^{34}S$ values in the range of +8‰ to +12‰ (Table 2; Fig. 7A), which are obviously different from those of mantle-derived magmatic sulfur (~0‰; Chaussidon et al., 1989). Devonian to Permian sedimentary rocks in the mining fields contain sedimentary sulfate such as gypsum and barite that have $\delta^{34}S$ values of ~+15‰ and +22‰ to +28‰, respectively (Jin, 2008; Liu and Lin, 1999), similar to that of Devonian to Permian seawater sulfates (+15 to +25‰; Claypool et al., 1980; Seal, 2006). Because $\Delta^{34}S_{sulfate-sulfide}$ could be up to +10 to +15‰ in Mississippi Valley-type Zn–Pb mineralizing systems (Machel et al., 1995; Ohmoto and Goldhaber, 1997; Ohmoto et al., 1990), the sulfur isotope signature of the deposit indicates that sulfur in the ores may have been derived predominantly by the reduction of sulfate derived from evaporite rocks in host strata (Basuki et al., 2008; Han et al., 2007).

6.2. Pb isotope constrain on possible sources of ore forming metals

Although some studies suggested that the metals of the Shaojiwan Pb–Zn deposit were provided by the Devonian to Permian carbonate rocks (Zhang et al., 2011), other studies of the SYG province suggested that Sinian to Carboniferous sedimentary rocks were important sources of metals (Li et al., 1999). In addition, Jin (2008) referred that metals were derived from Proterozoic basement rocks (such as Kunyang Group), whereas Zhou et al. (2001) considered that metals were provided by Neoproterozoic volcanic rocks.

Contents of U and Th for the sulfide minerals are too low to influence the Pb isotope compositions, whereas contrasted whole rocks of basalts, sedimentary and basement rocks need to be adjusted (e.g., Carr et al., 1995; Zhang et al., 2002). The Shaojiwan Pb–Zn deposit has homogeneous Pb isotope compositions (Table 3), unlike the adjusted Permian Emeishan flood basalts, Sinian to Permian carbonate rocks and Proterozoic basement rocks (Table 5). In the plot of $^{206}Pb/^{204}Pb$ vs. $^{207}Pb/^{204}Pb$ (Fig. 8), all samples from the Shaojiwan deposit fall close to the upper crust Pb evolution curve of Zartman and Doe (1981), within the field for basement rocks and near to the field for Devonian to Permian carbonate rocks. However, they are very different from the Permian Emeishan flood basalts and Sinian Dengying Formation, and more radiogenic than lead from the Tianqiao deposit (Fig. 8; Table 5). The data indicates that lead from the Shaojiwan deposit is most consistent with derivation mainly from basement rocks, whereas the Tianqiao lead probably came from a mixed source (Zhou et al., in press).

6.3. Evolution of hydrothermal fluids

Strontium isotopes of hydrothermal minerals are useful in tracing pathways of ore forming fluids (e.g., Deng et al., 2000; Fontbote and Gorzawski, 1990; Gromek et al., 2012; Zhou et al., 2001). However, they need to be corrected based on their closed age. Previous studies have yielded a hydrothermal calcite Sm–Nd age of the Huize Pb–Zn deposit of 222 ± 14 Ma (Li et al., 2007) and sulfide Rb–Sr ages of the Paoma and Tianqiao Pb–Zn deposits are 200.1 ± 4.0 Ma (Lin et al.,

Table 4
Rb and Sr isotope compositions of sphalerite from the Shaojiwan Pb-Zn deposit.

No.	Object	$Rb/10^{-6}$	$Sr/10^{-6}$	$^{87}Rb/^{86}Sr$	$^{87}Sr/^{86}Sr$ (2σ)	$(^{87}Sr/^{86}Sr)_t$	Source
SJW-9-2	Sphalerite	0.130	9.58	0.039	0.7114 ± 0.0001	0.7113	This
SJW-6		0.124	10.6	0.034	0.7119 ± 0.0001	0.7118	paper
SJW-1		0.124	7.57	0.048	0.7130 ± 0.0001	0.7129	
SJW-11		0.220	14.6	0.044	0.7114 ± 0.0001	0.7113	
SJW-7		0.203	10.6	0.055	0.7128 ± 0.0001	0.7126	

Note: $(^{87}Sr/^{86}Sr)_t = (^{87}Sr/^{86}Sr)_p - ^{87}Rb/^{86}Sr\ (e^{\lambda t} - 1)$, $\lambda_{Rb} = 1.41 \times 10^{-11} t^{-1}$, $t = 200$ Ma.

Table 5
Comparison of Pb isotope compositions of sulfide from the Shaojiwan Pb–Zn deposit with other geologic bodies in the SYG province, SW China.

Obj.		Num.	$(^{206}Pb/^{204}Pb)_{200\ Ma}$		$(^{207}Pb/^{204}Pb)_{200\ Ma}$		$(^{208}Pb/^{204}Pb)_{200\ Ma}$	
			Range	Mean	Range	Mean	Range	Mean
Shaojiwan Pb–Zn deposit		7	18.616–18.686	18.655	15.682–15.728	15.710	39.067–39.181	39.136
Minerals	Pyrite	3	18.620–18.661	18.645	15.694–15.714	15.705	39.075–39.144	39.120
	Sphalerite	3	18.616–18.686	18.658	15.682–15.728	15.712	39.067–39.181	39.142
	Galena	1	18.678		15.719		39.165	
Tianqiao Pb–Zn deposit		33	18.378–18.601	18.506	15.519–15.811	15.716	38.666–39.571	38.975
Minerals	Galena	26	18.378–18.601	18.505	15.519–15.811	15.715	38.666–39.571	38.991
	Sphalerite	5	18.506–18.526	18.516	15.713–15.731	15.722	38.901–38.983	38.942
	Pyrite	2	18.481–18.527	18.504	15.708–15.725	15.717	38.875–38.930	38.902
Lower Permian Qixia Fm., limestone		12	18.189–18.759	18.474	15.609–16.522	16.066	38.493–38.542	38.518
Upper Carboniferous Huanglong Fm., dolostone		12	18.136–18.167	18.152	15.656–16.675	15.666	38.204–38.236	38.220
Lower Carboniferous Baizuo Fm., dolostone		28	18.120–18.673	18.380	15.500–16.091	15.743	38.235–39.685	38.777
Lower Carboniferous Dapu Fm., dolostone		15	18.397–18.828	18.596	15.537–16.499	15.804	38.463–39.245	38.885
Upper Devonian Zaige Fm., limestone		13	18.245–18.842	18.542	15.681–16.457	16.012	38.715–39.562	38.998
Upper Sinian Dengying Fm., dolostone		20	18.198–18.517	18.360	15.699–15.987	15.818	38.547–39.271	38.909
Basement rocks (Kunyang Group)		27	17.781–20.993	18.789	15.582–15.985	15.686	37.178–40.483	38.427
Basement rocks (Huili Group)		16	18.094–18.615	18.287	15.630–15.827	15.708	38.274–38.932	38.585
Permian Emeishan flood basalts		56	18.175–19.019	18.541	15.528–15.662	15.574	38.380–39.928	38.983

Note: Pb isotope compositions of the Tianqiao Pb–Zn deposit are from Zhou et al. (in press), other data are from Zheng and Wang (1991), Hu (1999), Liu and lin (1999), Zhou et al. (2001), Huang et al. (2004) and this study. $(^{206}Pb/^{204}Pb)_t=(^{206}Pb/^{204}Pb)_p-\mu(e^{\lambda t}-1)$, $(^{207}Pb/^{204}Pb)_t=(^{207}Pb/^{204}Pb)_p-\mu/137.88(e^{\lambda' t}-1)$, $(^{208}Pb/^{204}Pb)_t=(^{208}Pb/^{204}Pb)_p-\omega(e^{\lambda'' t}-1)$, $\lambda=1.55125\times10^{-10}t^{-1}$, $\lambda'=9.8485\times10^{-10}t^{-1}$, $\lambda''=0.49475\times10^{-10}t^{-1}$, $t=200$ Ma.

2010) and 191.9 ± 6.9 Ma (Zhou et al., in press), respectively. Therefore, an age of ~200 Ma is considered to be the best timing of Pb–Zn mineralization in the SYG province.

Initial $(^{87}Sr/^{86}Sr)_{200\ Ma}$ ratios of sphalerite from the Shaojiwan Pb–Zn deposit range from 0.7113 to 0.7129 (Table 4), significantly higher than ratios of Permian Emeishan flood basalt (0.7039 to 0.7078, N = 85; Huang et al., 2004) and Sinian to Permian sedimentary (0.7073 to 0.7111; Table 6). In contrast, Proterozoic basement rocks have $^{87}Sr/^{86}Sr_{200\ Ma}$ (0.7243 to 0.7288) that are significantly higher than the ores (Table 6). Neither the older basement nor the younger burial rocks match the ore $^{87}Sr/^{86}Sr$ ratios, and so either there is a third source not considered in this study, or the ore strontium was sourced from a mixture of radiogenic Sr-enriched basement and radiogenic Sr-depleted Sinian to Permian sedimentary rocks.

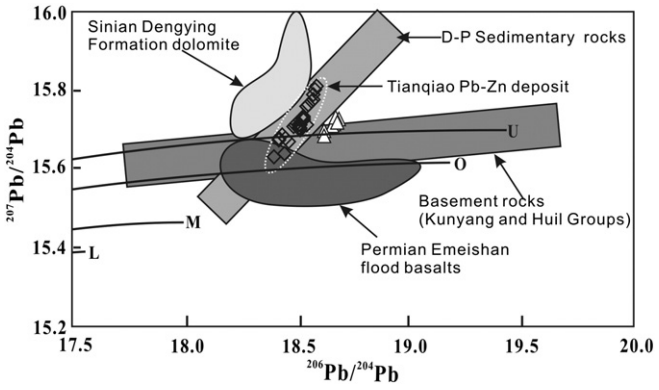

Fig. 8. Plot of $^{207Pb}/^{204}Pb$ vs. $^{206}Pb/^{204}Pb$ for the Shaojiwan Pb–Zn deposit. Trends for the upper crust (U), orogenic belt (O), mantle (M) and lower crust (L) are taken from Zartman and Doe (1981). Pb isotopic ratios of the Tianqiao Pb–Zn deposit are taken from Zhou et al. (in press). Sources of other data are taken from Hu (1999), Zhou et al. (2001, in press), Huang et al. (2004), Jin (2008) and this study.

7. Conclusions

1. The Shaojiwan Pb–Zn deposit is hosted in Devonian and Permian carbonate rocks and structurally controlled by the Yadu–Mangdong thrust fault. Lead–zinc ores occur as brecciated, veinlets and disseminations in dolomitized limestone rocks.
2. Sulfur in the hydrothermal fluids was derived predominantly from evaporite rocks in the host strata and Pb metal in the ore-forming solutions was originated mainly from the basement rocks, where the ore strontium was sourced from a mixture of the older basement rocks and the younger cover sequences.

Table 6
Sr isotope compositions of sphalerite, sedimentary rocks and basalts in the SYG province, SW China.

Object	Num.	$(^{87}Sr/^{86}Sr)_{200\ Ma}$		Source
		Range	Mean	
Sphalerite from Shaojiwan deposit	5	0.7113–0.7129	0.7120	This paper
Lower Permian Qixia Fm., limestone	3	0.7073–0.7089	0.7075	Zhou et al. (in press)
Upper Carboniferous Maping Fm., limestone	2	0.7099–0.7100	0.7100	Zhou et al. (in press)
Lower Carboniferous Baizuo Fm., dolostone	5	0.7087–0.7101	0.7094	This paper and Hu (1999)
Upper Devonian Zaige Fm., limestone	2	0.7084–0.7088	0.7086	Zhou et al. (in press)
Middle Devonian Haikou Fm., sandstone	2	0.7101–0.7111	0.7105	Deng et al. (2000); Zhou et al.
Upper Sinian Dengying Fm., dolostone	2	0.7083–0.7096	0.7089	(in press)
Permian Emeishan flood basalts	85	0.7039–0.7078	0.7058	Cong (1988); Li and Qin (1988);
Basement rocks	5	0.7243–0.7288	0.7268	Chen and Ran (1992); Huang et al. (2004)

Note: $(^{87}Sr/^{86}Sr)_t=(^{87}Sr/^{86}Sr)_p-{}^{87}Rb/^{86}Sr\ (e^{\lambda t}-1)$, $\lambda_{Rb}=1.41\times10^{-11}t^{-1}$, $t=200$ Ma.

Acknowledgment

This research was financially supported by the National Natural Science Foundation of China (nos. 41102055 and 41102053). Thanks are given to Dr. Jian-Feng Gao and Prof. Mei-Fu Zhou and Lin Ye for their insight suggestions. Comments and suggestions from Prof. Graham Carr, David Huston, Robert Ayuso and Kreeti Saravanan greatly improved the quality of the paper.

References

Basuki, N.I., Taylor, B.E., Spooner, E.T.C., 2008. Sulfur isotope evidence for thermochemical reduction of dissolved sulfate in Mississippi valley type zinc–lead mineralization, Bongara area, northern Peru. Economic Geology 103, 183–799.

Belshaw, N.S., Freedman, P.A., O'Nions, R.K., Frank, M., Guo, Y., 1998. A new variable dispersion double-focusing plasma mass spectrometer with performance illustrated for Pb isotopes. International Journal of Mass Spectrometry 181, 51–58.

Carr, G.R., Dean, J.A., Suppel, D.W., Heithersay, P.S., 1995. Precise lead isotope fingerprinting of hydrothermal activity associated with Ordovician to Carboniferous metallogenic events in the Lachlan fold belt of New South Wales. Economic Geology 90, 1467–1505.

Chaussidon, M., Albarède, F., Sheppard, S.M.F., 1989. Sulphur isotope variations in the mantle from ion microprobe analyses of micro-sulphide inclusions. Earth and Planetary Science Letters 92, 144–156.

Chen, H.S., Ran, C.Y., 1992. Isotope Geochemistry of Copper Deposit in Kangdian Area. Geological Publishing House, Beijing, pp. 1–25 (in Chinese).

Claypool, G.E., Holser, W.T., Kaplan, I.R., Sakai, H., Zak, I., 1980. The age curves of sulfur and oxygen isotopes in marine sulfate and their mutual interpretation. Chemical Geology 28, 199–260.

Cong, B.L., 1988. Evolution and Formation of Panxi Rift. Science Press, Beijing, pp. 10–33 (in Chinese).

Cromie, P.W., Gosse, R.R., Zhang, P., Zhu, X., 1996. Exploration for Carbonate-hosted Pb–Zn Deposits, Sichuan, P.R.C. [abs.]: International Geological Congress, 30th, Beijing, China, p. 412 (Abstracts).

Deng, H.L., Li, C.Y., Tu, G.Z., Zhou, Y.M., Wang, C.W., 2000. Strontium isotope geochemistry of the Lemachang independent silver ore deposit, northeastern Yunnan, China. Science in China (Series D): Earth Science 43, 337–346.

Deol, S., Deb, M., Large, R.R., Gilbert, S., 2012. LA-ICPMS and EPMA studies of pyrite, arsenopyrite and loellingite from the Bhukia–Jagpura gold prospect, southern Rajasthan, India: implications for ore genesis and gold remobilization. Chemical Geology 326–327, 72–87.

Dixon, G., Davidson, G.J., 1996. Stable isotope evidence for thermochemical sulfate reduction in the Dugald River (Australia) strata-bound shale-hosted zinc–lead deposit. Chemical Geology 129, 227–246.

Fontbote, L., Gorzawski, H., 1990. Genesis of the Mississippi valley-type Zn–Pb deposit of San Vicente, central Peru: geologic and isotopic (Sr, O, C, S, Pb) evidence. Economic Geology 85, 1402–1437.

Gromek, P., Gleeson, S.A., Simonetti, A., 2012. A basement-interacted fluid in the N81 deposit, Pine Point Pb–Zn district, Canada: Sr isotopic analyses of single dolomite crystals. Mineralium Deposita 47, 749–754.

Haest, M., Schneider, J., Cloquet, C., Latruwe, K., Vanhaecke, F., Muchez, P., 2010. Pb isotopic constraints on the formation of the Dikulushi Cu–Pb–Zn–Ag mineralisation, Kundelungu Plateau (Democratic Republic of Congo). Mineralium Deposita 45, 393–410.

Han, R.S., Liu, C.Q., Huang, Z.L., Chen, J., Ma, D.Y., Lei, L., Ma, G.S., 2007. Geological features and origin of the Huize carbonate-hosted Zn–Pb–(Ag) District, Yunnan, South China. Ore Geology Reviews 31, 360–383.

Hu, Y.G., 1999. Ag occurrence, source of ore-forming metals and mechanism of Yinchangpo Ag–Pb–Zn deposit, Guizhou. Ph.D. Thesis. Institute of Geochemistry, Chinese Academy of Sciences, pp. 10–55 (in Chinese with English abstract).

Huang, Z.L., Li, W.B., Chen, J., Han, R.S., Liu, C.Q., Xu, C., Guan, T., 2003. Carbon and oxygen isotope constraints on the mantle fluids join the mineralization of the Huize super-large Pb–Zn deposits, Yunnan Province, China. Journal of Geochemistry Exploration 78 (79), 637–642.

Huang, Z.L., Chen, J., Han, R.S., Li, W.B., Liu, C.Q., Zhang, Z.L., Ma, D.Y., Gao, D.R., Yang, H.L., 2004. Geochemistry and Ore-formation of the Huize Giant Lead–zinc Deposit, Yunnan Province, China: Discussion on the Relationship between the Emeishan Flood Basalts and Lead–zinc Mineralization. Geological Publishing House, Beijing, pp. 1–214 (in Chinese).

Huang, Z.L., Li, X.B., Zhou, M.F., Li, W.B., Jin, Z.G., 2010. REE and C–O isotopic geochemistry of calcites from the word-class Huize Pb–Zn deposits, Yunnan, China: implication for the ore genesis. Acta Geologica Sinica (English edition) 84, 597–613.

Huston, D.L., Sie, S.H., Suter, G.F., Cooke, D.R., Both, R.A., 1995. Trace elements in sulfide minerals from Eastern Australian volcanic-hosted massive sulfide deposits: part 1. Proton microprobe analyses of pyrite, chalcopyrite, and sphalerite, and part 2. Selenium levels in pyrite: comparison with $\delta^{34}S$ values and implications for the source of sulfur in volcanogenic hydrothermal systems. Economic Geology 90, 1167–1196.

Jin, Z.G., 2008. The ore-control factors, ore-forming regularity and forecasting of Pb–Zn deposit. Northwestern Guizhou Province. Engine Industry Press, Beijing, pp. 1–105 (in Chinese).

Large, R.R., Bull, S.W., McGoldrick, P.J., 2000. Lithogeochemical halos and geochemical vectors to stratiform sediment hosted Zn–Pb–Ag deposits part 2. HYC deposit, McArthur River, northern Territory. Journal of Geochemical Exploration 68, 105–126.

Leach, D.L., Bradley, D.C., Huston, D., Pisarevsky, S.A., Taylor, R.D., Gardoll, S.J., 2010. Sediment-hosted lead–zinc deposits in Earth history. Economic Geology 105, 593–625.

Li, F.H., Qin, J.M., 1988. Presinian System in Kangdian Area. Chongqing Press, Chongqing, pp. 15–45 (in Chinese).

Li, L.J., Liu, H.T., Liu, J.S., 1999. A discussion on the source bed of Pb–Zn–Ag deposits in northeast Yunnan. Geological Exploration for Non-ferrous Metals 8, 333–339 (in Chinese with English abstract).

Li, Q.L., Chen, F.K., Wang, X.L., Li, C.F., 2005. Ultra-low procedural blank and the single grain mica Rb–Sr isochron dating. Chinese Science Bulletin 50, 2861–2865.

Li, W.B., Huang, Z.L., Yin, M.D., 2007. Dating of the giant Huize Zn–Pb ore field of Yunnan province, southwest China: constrains from the Sm–Nd system in hydrothermal calcite. Resource Geology 57, 90–97.

Liao, W., 1984. A discussion on the S and Pb isotopic composition characteristics and metallogenic model of the Pb–Zn ore zones in eastern Yunnan and western Guizhou. Journal of Geology and Exploration 1, 1–6 (in Chinese with English abstract).

Lin, Z.Y., Wang, D.H., Zhang, C.Q., 2010. Rb–Sr isotopic age of sphalerite from the Paoma lead–zinc deposit in Sichuan Province and its implications. Geology in China 37, 488-494 (in Chinese with English abstract).

Liu, H.C., Lin, W.D., 1999. Study on the Law of Pb–Zn–Ag Ore Deposit in Northeast Yunnan, China. Yunnan University Press, Kunming, pp. 1–468 (in Chinese).

Machel, H.G., Krouse, H.R., Sassen, R., 1995. Products and distinguishing criteria of bacterial and thermochemical sulfate reduction. Applied Geochemistry 10, 373–389.

Ohmoto, H., Goldhaber, M.B., 1997. Sulfur and carbon isotopes, In: Barnes, H.L. (Ed.), Geochemistry of Hydrothermal Ore Deposits, 3rd ed. Wiley, New York, pp. 517–611.

Ohmoto, H., Kaiser, C.J., Geer, K.A., 1990. Systematics of sulphur isotopes in recent marine sediments and ancient sediment-hosted base metal deposits. In: Herbert, H.K., Ho, S.E. (Eds.), Stable Isotopes and Fluid Processes in Mineralization: Geol Dep Univ Extens Univ Western Australia, 23, pp. 70–120.

Powell, T.G., Macqueen, R.W., 1984. Precipitation of sulfide ores and organic matter: sulfate reactions at Pine Point, Canada. Science 224, 63–66.

Qiu, Y.M., Gao, S., McNaughton, N.J., Groves, D.I., Ling, W.L., 2000. First evidence of >3.2 Ga continental crust in the Yangtze craton of south China and its implications for Archean crustal evolution and Phanerozoic tectonics. Geology 28, 11–14.

Seal, I.R., 2006. Sulfur isotope geochemistry of sulfide minerals. Review of Mineralogy and Geochemistry 61, 633–677.

Sun, W.H., Zhou, M.F., Gao, G.F., Yang, Y.H., Zhao, X.F., Zhao, J.H., 2009. Detrital zircon U–Pb geochronological and Lu–Hf isotopic constraints on the Precambrian magmatic and crustal evolution of the western Yangtze Block, SW China. Precambrian Research 172, 99–126.

Sverjensky, D.A., 1981. The origin of a Mississippi valley-type deposit in the Viburnum Trend, south Missouri. Economic Geology 76, 1848–1872.

Tu, G.C., 1984. Geochemistry of Strata-bound Ore Deposits in China (Volumes I). Science Press, Beijing, pp. 13–69 (in Chinese with English abstract).

Wilkinson, J.J., Eyre, S.L., Boyce, A.J., 2005. Ore-forming processes in Irish-type carbonate-hosted Zn–Pb deposits: evidence from mineralogy, chemistry, and isotopic composition of sulfides at the Lisheen Mine. Economic Geology 100, 63–86.

Xie, J.R., 1963. Introduction of the Chinese Ore Deposits. Scientific Books Publishing House, Beijing, pp. 1–71 (in Chinese).

Yan, D.P., Zhou, M.F., Song, H.L., Wang, X.W., Malpas, J., 2003. Origin and tectonic significance of a Mesozoic multi-layer over-thrust system within the Yangtze Block (South China). Tectonophysics 361, 239–254.

Ye, L., Cook, N.J., Ciobanu, C.L., Liu, Y.P., Zhang, Q., Liu, T.G., Gao, W., Yang, Y.L., Danyushevsky, L., 2011. Trace and minor elements in sphalerite from base metal deposits in South China: a LA-ICPMS study. Ore Geology Reviews 39, 188–217.

Zartman, R.E., Doe, B.R., 1981. Plumbotectonics—the model. Tectonophysics 75, 135–162.

Zhang, Q., Liu, J.J., Shao, S.X., 2002. An estimate of the lead isotopic compositions of upper mantle and upper crust and implications for the source of lead in the Jinding Pb–Zn deposit in western Yunnan, China. Geochemical Journal 36, 271–287.

Zhang, Z., Huang, Z.L., Zhou, J.X., Li, X.B., Jin, Z.G., Zhang, L.W., 2011. Sulfur isotope geochemistry of Shaojiwan Pb–Zn Deposit in Northwest Guizhou, China. Acta Mineralogica Sinica 31, 496–501 (in Chinese with English abstract).

Zhao, X.F., Zhou, M.F., Li, J.W., Sun, M., Gao, J.F., Sun, W.H., Yang, J.H., 2010. Late Paleoproterozoic to early Mesoproterozoic Dongchuan Group in Yunnan, SW China: implications for tectonic evolution of the Yangtze Block. Precambrian Research 182, 57–69.

Zheng, M.H., Wang, X.C., 1991. Genesis of the Daliangzi Pb–Zn deposit in Sichuan, China. Economic Geology 86, 831–846.

Zhou, C.X., Wei, C.S., Guo, J.Y., 2001. The source of metals in the Qilingchang Pb–Zn deposit, Northeastern Yunnan, China: Pb–Sr isotope constraints. Economic Geology 96, 583–598.

Zhou, M.F., Yan, D.P., Kennedy, A.K., Li, Y.Q., Ding, J., 2002. SHRIMP zircon geochronological and geochemical evidence for Neo-proterozoic arc-related magmatism along the western margin of the Yangtze Block, South China. Earth and Planetary Science Letters 196, 1–67.

Zhou, J.X., Huang, Z.L., Zhou, G.F., Li, X.B., Ding, W., Bao, G.P., 2010. Sulfur isotopic compositions of the Tianqiao Pb–Zn ore deposit, Guizhou Province, China: implications for the source of sulfur in the ore-forming fluids. Chinese Journal of Geochemistry 29, 301–306.

Zhou, J.X., Huang, Z.L., Zhou, G.F., Li, X.B., Ding, W., Bao, G.P., 2011. Trace elements and rare earth elements of sulfide minerals in the Tianqiao Pb–Zn ore deposit, Guizhou Province, China. Acta Geologica Sinica (English edition) 85, 189–199.

Zhou, J.X., Huang, Z.L., Zhou, M.F., Li, X.B., Jin, Z.G., Constraints of C–O–S–Pb isotope compositions and Rb–Sr isotopic age on the origin of the Tianqiao carbonate-hosted Pb–Zn deposit, SW China. Ore Geology Reviews, in press. http://dx.doi.org/10.1016/j.oregeorev.2013.01.001.